MITSUBISHI ELECTRIC R&D CENTRE EUROPE

18th European Conference on Power Electronics and Applications (EPE'16 ECCE Europe) , Sept. 16

DOI: 10.1109/EPE.2016.7695517

A 2W, 5MHz, PCB-integration compatible 2.64cm^{3}regulated and isolated power supply for gate driver

N. Degrenne
G. Lefevre
S. Mollov

A 2W, 5MHz, PCB-Integration Compatible 2.64cm^3 Regulated and Isolated Power Supply for Gate Driver

DEGRENNE Nicolas, LEFEVRE Guillaume, MOLLOV Stefan
Mitsubishi Electric R&D Centre Europe (MERCE)
1, allée de Beaulieu
Rennes, France
E-Mail: n.degrenne@fr.merce.mee.com
URL: http://www.mitsubishielectric-rce.eu/

Keywords

«Power supply», «Resonant converter», «Gallium Nitride (GaN)», «System integration», «Passive component integration».

Abstract

This paper presents an isolated power supply unit for high-side gate driver. It generates a bipolar voltage level (+15V/-5V) and an auxiliary voltage level of +5V. The LLC topology is used at fixed frequency of 5MHz. A voltage control based on switched resonant tank is used to compensate voltage drops in the converter at high load currents. This new control strategy allows using a simple feedback loop where isolation is performed by a control transformer which is integrated with the main power transformer. The paper thus demonstrates a custom concentric planar dual transformer. Its magnetic material is made with molded ferrite/epoxy composite. The magnetic material is formed in situ with a low-temperature PCB-compatible process. The other components of the converter are off-the-shelf discrete components. The supply is implemented with GaN MOSFETs that allow higher efficiency and better output voltage control than Si devices at high switching frequency. The power supply is built as a stack of 3 PCBs, has a power density of 0.76W/cm^3 (12.45W/In^3), and is intended to be part of the design of highly integrated PCB-based converters.

Introduction

With new PCB-based technologies entering the market (e.g. power die embedding) [1], the interest is rising in PCB-process compatible gate drivers. The perspective of having a gate driver, the corresponding supply and power devices integrated in the same PCB process would allow cost reduction and higher power density.

High-side switch gate drivers require isolated voltage supply. The market penetration of fast devices such as WBG (wide band gap) imposes more constraints, i.e. bipolar voltage operation, and high dV/dt immunity [2]. When considering kW-level power converters, the volume and cost of the supply can be higher than the power semiconductor device itself. There is therefore a need for Watt-level, small, low-cost, isolated and bipolar supply with high dV/dt immunity.

In the literature, Watt-level isolated power supplies exhibit different level of integration. In [3], a system in package 0.5W power supply using coreless transformers is presented. This is made possible by operation at 170MHz. The maximum efficiency is 33%. Another supply in a system in package is presented in [4], but with a transformer on silicon with magnetic core. The rated power is 1W, the operating frequency is 1MHz, and the maximum efficiency is 55%.

The design of integrated high-frequency transformers is a research topic by itself. A comprehensive literature review is done in [5]. Two main types of architectures can be distinguished: either the windings are planar (i.e. 2D) [3, 4, 6, 7, 8] or the magnetic material is planar [9, 10, 11, 12]. Two main types of magnetic cores can be distinguished: either the conventional method where the cores are built in a specific process and assembled later [4, 6], or a more integrated method where the core is formed in place [7, 8, 9, 10, 11, 12]. This method needs to be low-temperature in order to comply with the process of PCB.

The objective of this paper is to present a 2W, 5MHz, 2.64cm^3 regulated and isolated power supply unit for gate driver supply that demonstrates formed-in-place magnetic component integration. First, the general design is described and the active discrete components are selected. Then, an original control strategy is introduced. Next, the custom planar transformer with its composite magnetic core is presented. Finally, experimental results are provided.

Topology design and active component selection

Specifications

The specifications are summarized in Table I. The input voltage V_{IN} is 12V. The power supply is able to generate 2 bipolar output voltage levels of +15V and -5V with 50mA nominal current (e.g. to drive SiC devices), and an auxiliary output voltage level of +5V with 200mA nominal current (e.g. to supply sensors, analog or digital circuits for the purpose of gate trajectory control or condition monitoring). The bipolar supplies are supposed to be post-regulated (user-defined), and only the +5V requires accurate control of ±10%. A maximum isolation capacitance value of 10pF is a typical value for commercially available isolated 2W power supply units (e.g. Recom RxxP2xx product line). Figure 1 shows a picture of the converter.

Table I: Main specifications

Nominal input voltage	12V
Output voltage / current 1	+15V / 50mA
Output voltage / current 2	-5V / 50mA
Output voltage / current 3	+5V / 200mA
Load regulation (Max)	±10%
Isolation capacitance (max)	10pF

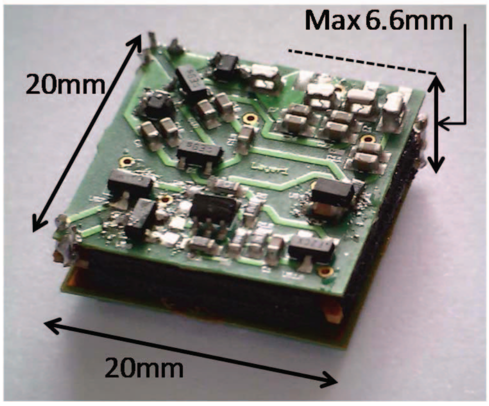

Figure 1 : Converter picture (output bridge on top)

Topology

A LLC series resonant topology was selected due to its soft-switching features and ability to operate with a passive output bridge (Fig. 2). This topology theoretically offers a noteworthy operating point with unitary gain irrespective of the load current when the switching frequency equals the resonant frequency. This operating point is used to decrease the requirements for output voltage regulation.

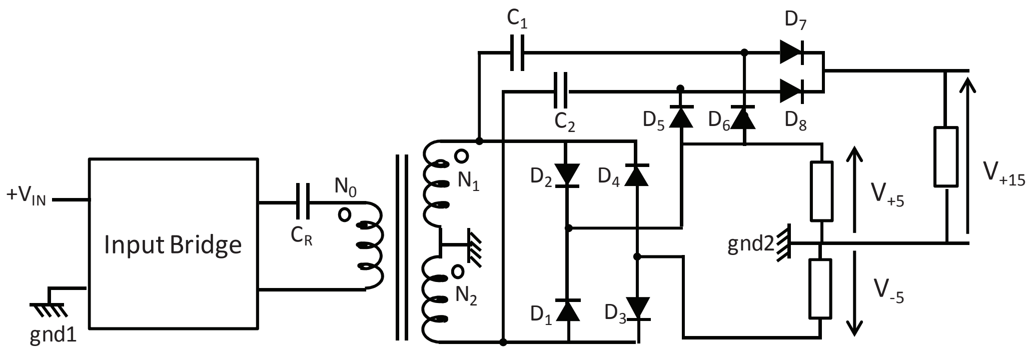

Figure 2 : Converter topology

The input bridge is a half-bridge. In a previous work, it was implemented with two high speed CMOS buffer ICs ISL55110 in parallel. Each IC is itself composed of two buffers in parallel. The relatively high on-resistance of 3Ω and output parasitic capacitance of 135pF mainly contributed to losses, leading to a poor efficiency in the order of 50% maximum. In addition the voltage regulation was difficult due to high voltage drops at high load. This paper therefore presents an implementation that uses 40V EPC8004 GaN devices and a suitable LM5113 driver. The MOSFETs and driver are low-footprint with bump interconnections. Fig. 3 shows the assembly of such devices. The footprint is very small, making it ideal for the application. The X-ray photograph (performed by TEAM31, France) shows the soldering areas. This implementation allows full benefit of the LLC topology with partial ZVS operation because the dead-times can be tuned and the output capacitances are low-enough to be significantly charged and discharged by the magnetizing current. One drawback however is the relatively high cost.

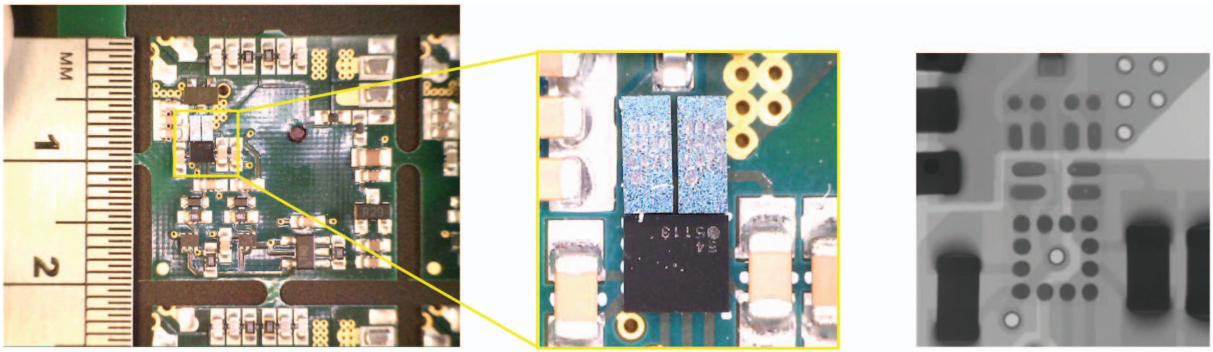

Fig. 3 Photograph of the GaN input bridge. From left to right: global view, zoom on the driver and 2 GaN MOSFETs, corresponding X-ray picture.

As shown in Fig. 2, the output bridge only uses Schottky diodes with low junction capacitances. References BAS4002 were selected for bipolar outputs with low-output current (i.e. D3, D4, D5, D6, D7, D8) and two extra HSMS270C were connected in parallel for the high-output current (i.e. D1, D2) because of better conduction characteristics. As such, the voltage drops across the diodes match at nominal current values and output voltages are balanced. The voltage +15V is generated with voltage doublers (C1, D5, D8 and C2, D6, D7) referenced to +5V. Capacitors C1 and C2 are 100nF X7R capacitors. The layout of the output bridge is visible in Fig. 1.

Control strategy with switched resonant tank

One challenge of Watt-level isolated converters is control because it has to comply with the isolation requirements. If the control is performed on the primary side (i.e. by modifying the switching frequency or pattern of the input bridge signal), an isolated feedback loop is required, for example using an optical isolation mean. An alternative way to perform output voltage control is to use LDO devices at each output, but it is detrimental for efficiency.

In this paper, the input bridge is operated at a fixed switching frequency of 5MHz and fixed duty-cycle of 0.5. Under these operating conditions, the gain of the converter is unitary irrespective of the load current since the resonant tank matches the switching frequency. However, due to the conduction losses, the voltage tends to decrease at high load. In addition to that, due to parasitic capacitances at the secondary, voltage tends to increase at low load. These are the reasons why a voltage regulation was implemented.

The control is based on a switched resonant tank. It discretely modifies the series resonant inductance to achieve two gain values for the converter (boundaries). The resonant tank is modified between these two states at a duty-cycle that allows reaching a gain value in between the two boundaries. Figure 4 illustrates the concept of switched resonant tank control. The output voltage +5V is scaled down and compared to a reference value. The bidirectional switch S is turned ON or OFF with a hysteresis law according to comparator output. When S is OFF, the inductor L_A is involved in the series resonant tank. When S is ON, L_A is short-circuited and the equivalent series inductor is lower, i.e. the resonant frequency is higher and equals the switching frequency (higher gain at high load current).

Figure 5 provides theoretical results obtained with the first harmonic approximation (FHA) and taking into consideration the conduction losses of the input bridge, transformers, and output voltage. With an active control of the switch S, the output voltage is controlled for all load current between the red and blue curves. The objective voltage of +5V±10% can thus be obtained for all load currents, which would not be the case otherwise.

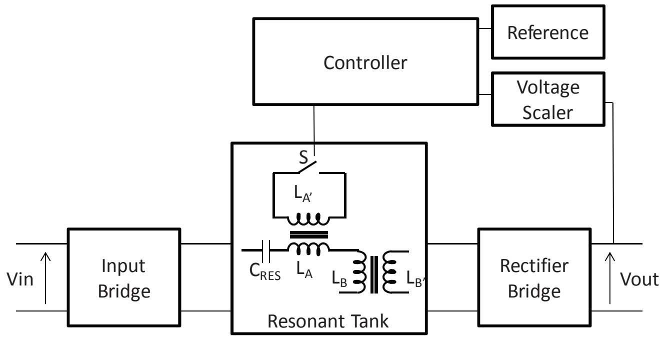

Figure 4: Switched resonant tank control schematic

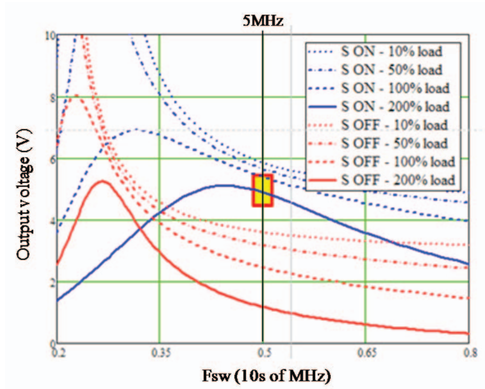

Figure 5: Simulated output voltage as a function of switching frequency when S is ON (blue) and OFF (red)

Transformer custom design and construction with composite magnetic material

The transformer is a critical component of the converter for several reasons: 1) according to the control strategy, two transformers are required, 2) a PCB-compatible process is required, 3) the use of discrete active components for the input and output bridges limits the switching frequency to 5MHz, and therefore, core-less transformers are out of specifications.

The design of the transformer was selected to generate two concentric planar transformers. The design methodology made use of FEM simulation (FEMM 4.2) and experimental tests of 3 different designs, with both polyimide and FR4 as dielectric material. Figure 6 shows the different windings of the selected design. All the windings (N0, N1, N2 and control windings) have 3 turns. The FR4 PCB is composed of 4 layers for a total thickness of 0.8mm. The four copper layers (final thickness of 35µm) are stacked with a 250µm core and two 205µm prepregs, providing a theoretical isolation voltage of 8kV. Conformal dielectric coating was sprayed on the two faces of the PCB before forming the magnetic core.

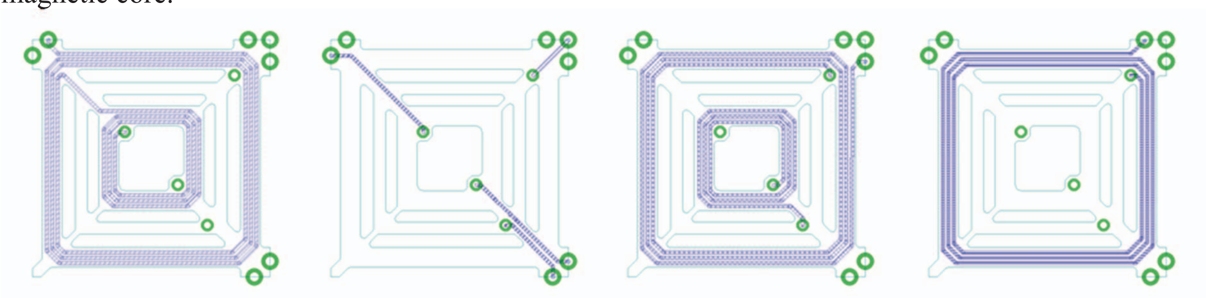

Figure 6: Copper design for the transformer, from left to right, copper layer from top to bottom

Since no magnetic component was available off-the-shelf for the considered dimensions, and to demonstrate a formed-in-place technology suitable for integration, a custom composite (ferrite/epoxy) magnetic material was molded around the PCB, and constitutes two distinct magnetic components, one for each transformer. This composite magnetic material is highly conformable and is cured at low temperature, compatible with PCB processes. Figure 7 illustrates process steps that were performed in the laboratory. The 3 different designs are shown on the left. First, a mold was milled into PTFE sheets. Then, ferrite powder (Ferroxcube 4F1) with fine grain obtained by sieving at 0.4mm holes was mixed with a low-viscosity epoxy resin (Electrolube EER1448RP250G) in a 6 to 1 volume ratio and used to fill the mold with the PCB windings in it. Then, the mold was closed and mechanical pressure was applied during drying above ambient temperature (80°C). Finally, the mold was removed.

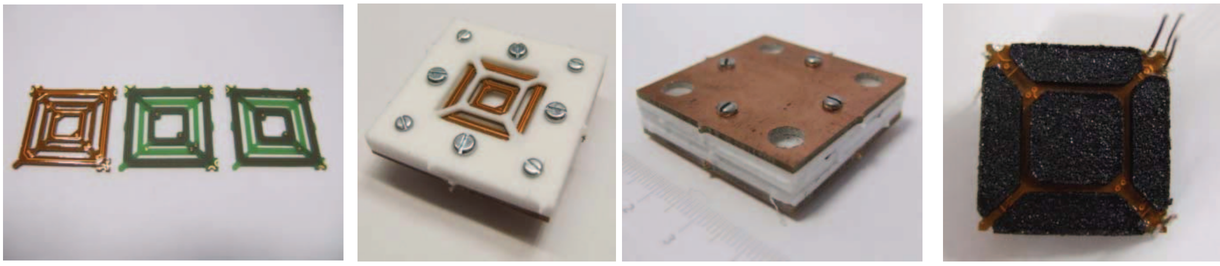

Figure 7 : Process for construction of the ferrite/epoxy composite magnetic material

As a result, a resonant inductance value of 403nH and 1172nH is obtained when switch S is respectively ON and OFF. The total inter-winding capacitance values between primary and secondary were experimentally extracted with an impedance meter and are in the order of 13pF. This value is slightly higher than the isolation capacitance of the typical commercially-available RECOM RxxP2xx series (10pF max) and should be further reduced to allow switching WBG devices at speeds higher than 10V/ns.

Results

The resulting supply is built as a stack of input PCB, transformer, and output PCB as depicted in Fig. 1. The connection between boards was made with low-profile connectors positioned in cut vias, on the periphery of the circuits. The length and width of 20mm are dictated by the transformer footprint. The height of 6.6mm is the sum of 3mm for transformer, 2x0.8mm for FR4 PCBs, 1mm for components on the input-bridge side and 1 mm on the output bridge side. Note that the package is not included in the volume because the target to reach with this supply is to be embedded into PCB process.

Experimental waveforms

The resonant capacitance that maximizes the auxiliary output voltage at nominal load when S is ON was selected. In other words, when S is ON, the resonance frequency equals the switching frequency of 5MHz. The corresponding capacitance value is 2840pF.
The dead-times were performed on the signal before amplification by the driver with simple RCD delays. The capacitor value was set to 100pF. The dead-times were increased to a reasonable value that allows partial ZVS, without needlessly altering the duty-cycle and input bridge voltage shape. Figure 8 shows the input bridge voltage with different values of delay resistor. A resistor value of 150Ω was finally chosen.

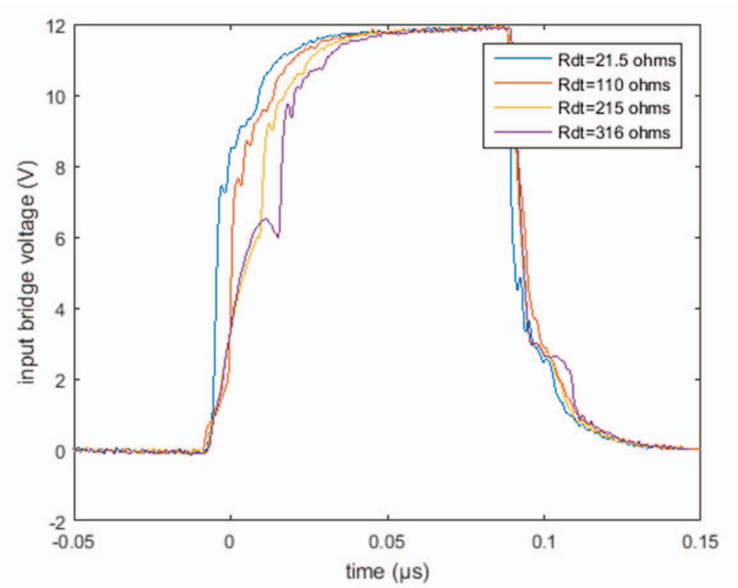

Figure 8: Input bridge voltage with several dead-times

Figure 9 shows experimental waveforms for two output current levels: low current (10% nominal) in blue and high current (nominal) in red. These curves were acquired with the control switch S being ON. At this operating point, the switching frequency perfectly matches the resonant frequency.
The resonant tank current was measured indirectly by deriving the voltage across the resonant capacitor.

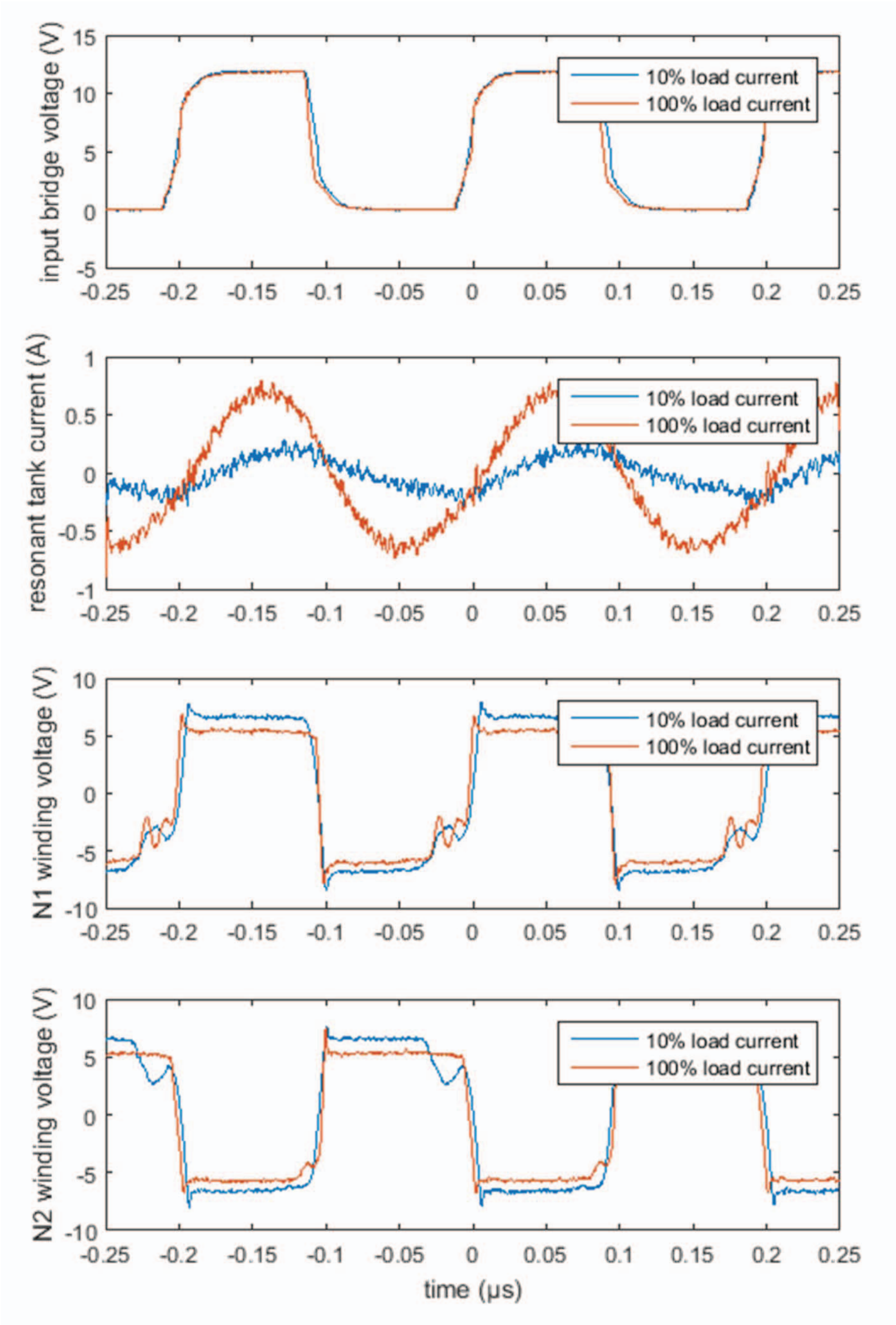

Figure 9: Experimental waveforms for two output current levels when S is ON, from top to bottom: input bridge voltage, resonant tank current, N1 winding voltage, N2 winding voltage

Control validation

The operation of the +5V control was first verified using balanced load currents for each output as illustrated in Fig. 10. As can be seen, for low output current, the output voltage Vaux (green curve) is above 5V due to the boost effect created by the parasitic capacitors at the secondary. This problem is mitigated by adding a Zener diode to clamp the +15V output. As a result, the +5V output is clamped to 5.8V maximum.
At 10% nominal load (i.e. 5mA from +15V and -5V outputs and 20mA from +5V output) and above, the output voltage equals 5V and the switch S starts switching with a linearly increasing duty-cycle. At 80% nominal load, switch S is always ON and the auxiliary voltage decreases down to 4.5V due to conduction losses.

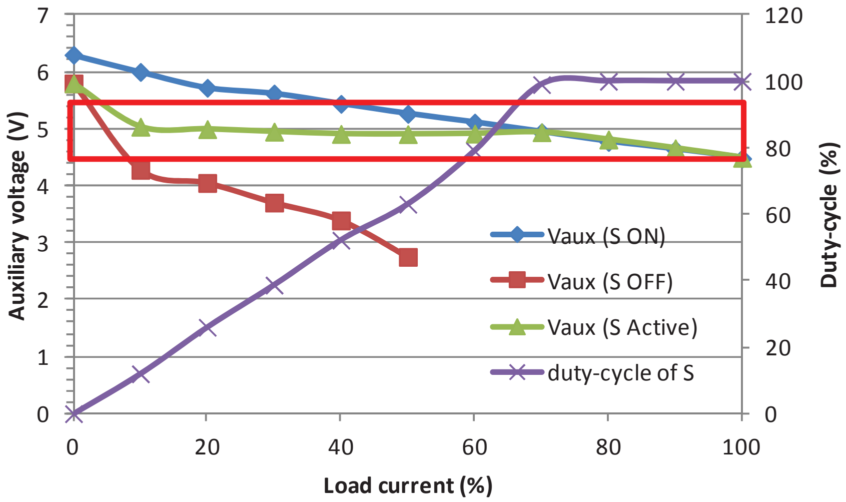

Figure 10: Output auxiliary voltage as a function of load current when S is ON (blue diamond), when S is OFF (red square), when S is controlled (green triangle), and duty-cycle of switch S (purple cross)

The control operation was then confirmed with unbalanced load currents on the bipolar output levels (+15V and -5V) and the auxiliary output levels (+5V). Figure 11 shows the auxiliary voltage, and the bipolar voltages +15V and -5V for several combinations of load currents. When high current is drawn from the +5V output while small current is drawn from the bipolar outputs, the bipolar voltages are higher than expected. This is not detrimental to the overall operation since the bipolar voltages will be post-regulated. For all combinations of load currents, the output voltages meet the specifications.

Loss analysis

Figure 12 shows the efficiency with respect to auxiliary load current for various values of bipolar current. Efficiency was measured to be 72%±2% at nominal load (2W). Maximum efficiency reaches 76.6% when the bipolar load current is 50mA and the auxiliary load current is 100mA. The efficiency measurements were performed with four Agilent U1240 current sensors and four Fluke 87V voltage sensors. The maximum error of ±2% on efficiency was calculated by considering the accuracy of each measure (expressed as % reading + number of least significant digit) for each used voltage and current range.

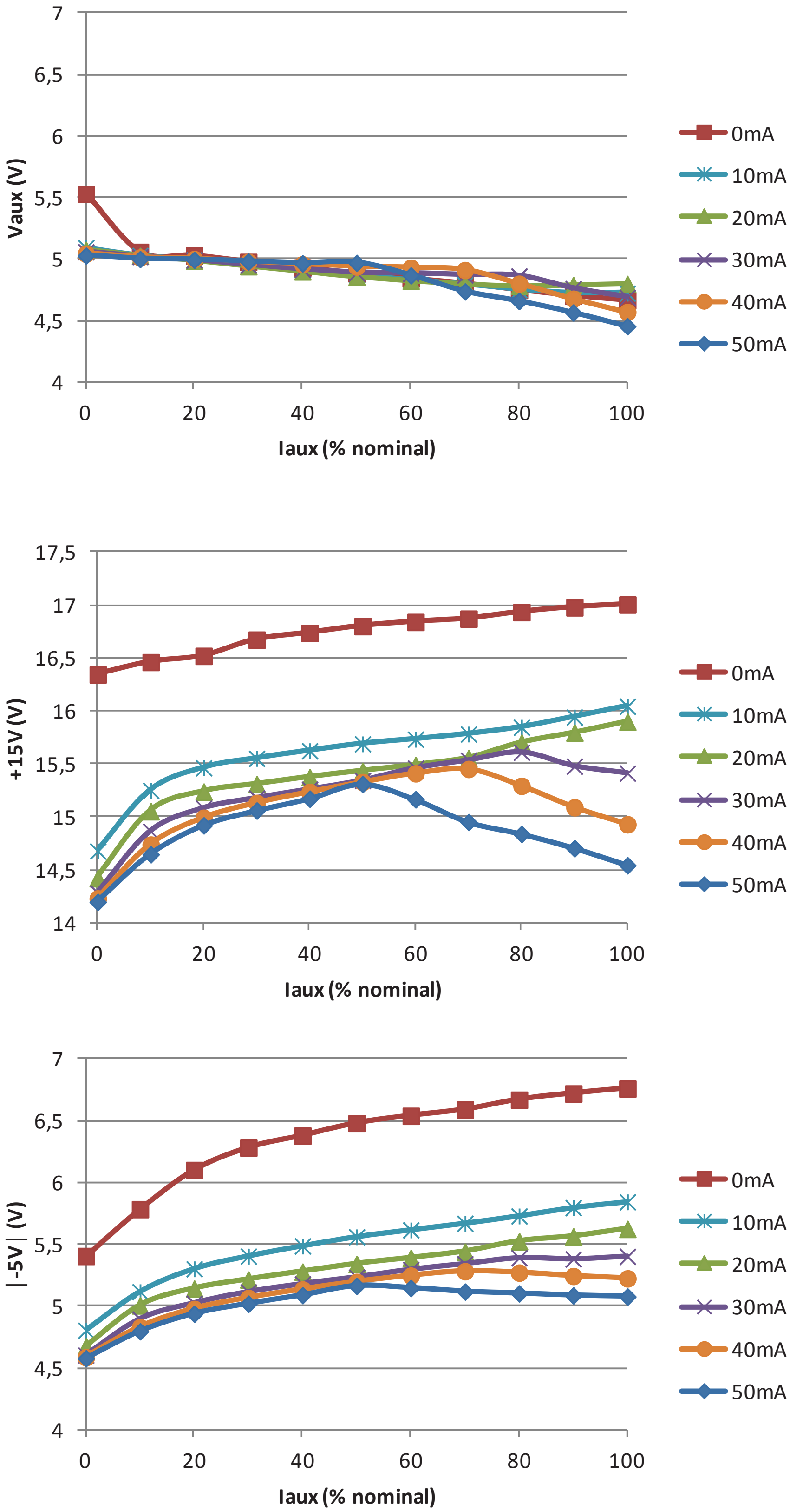

Figure 11: Output voltage as a function of auxiliary load current for different values of bipolar current when S is controlled

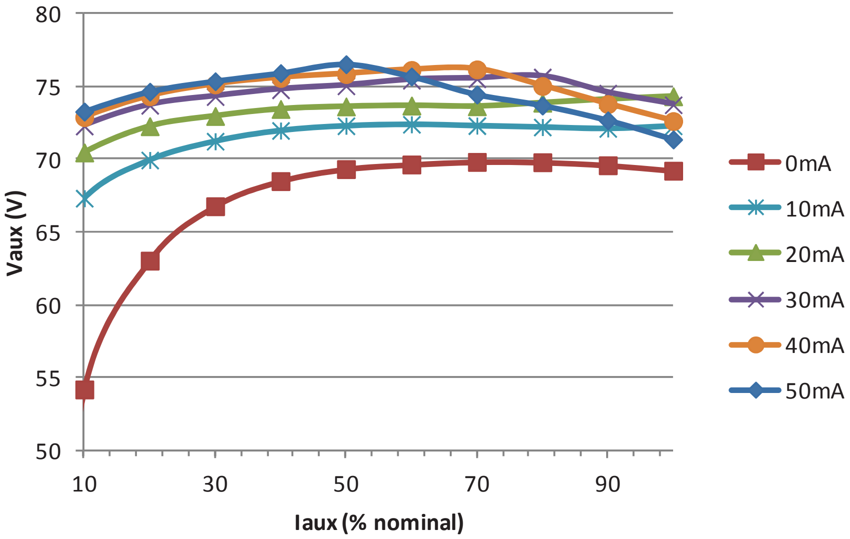

Figure 12: Efficiency as a function of auxiliary load current for different values of bipolar current

Natural convection was sufficient to cool down the power supply, and only minor increase of temperature was observed. Figure 13 shows that a maximum increase of 13°C exists at nominal load. It is located in the output bridge, in the rectifying diodes. The gate driver LM5113 is a visible hot spot on the input bridge. It is supplied by a +5V specific voltage source and draws 24.5mA. The gate driver supply was not included in the efficiency calculations. Because of their very low on-resistance, low Coss and partial ZVS operation, the GaN switches of the input bridge generate a small amount of losses. The transformer exhibits a homogeneous increase of temperature. This implies that a loss analysis dedicated to the transformer would be interesting, because if the high frequency copper losses (proximity and skin effects) can be reasonably estimated with FEM simulation, the custom composite magnetic material has unknown properties. One straight forward degree of freedom is the increase of copper thickness from 35µm to 70µm. However, mainly the losses stemming from the output bridge should be minimized. Synchronous rectification was initially rejected because of the high impact of parasitic capacitances on the output voltage at low load (boost effect).

Note that it was estimated that with dedicated custom input bridge IC in CMOS350nm technology, the losses could be low enough to compete the efficiency level obtained with GaN, at a lower cost. In addition, the switching frequency could be further increased, thus reaching a higher power density, therefore potentially outperforming state-of-the-art prototypes [3, 4, 5]. The implementation of the rectifying bridge in nano-scale CMOS technology would also be a valuable perspective.

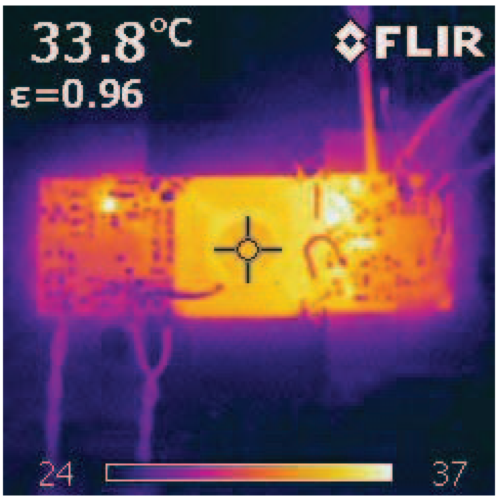

Figure 13: Infra-red picture of the unfolded supply (from left to right: input bridge, transformer, output bridge) at 100% nominal current

Conclusions and perspectives

A 2W, 5MHz, 2.64cm^3, isolated (8kV), bipolar, LLC power supply for high-side gate driver application was designed and tested. Two novel technologies were demonstrated to improve the integration level of the supply. First, the control of the auxiliary +5V output is performed with a switched resonant tank. This avoids using an isolated feedback loop or of an LDO. Secondly, the dual, concentric, and planar transformer was built with PCB technology and ferrite/epoxy composite magnetic cores. This design offers a low-volume transformer with a custom shape and form-factor. The composite magnetic cores perform as expected, but full material characterization would allow a complete optimization of the transformer design. One drawback of the planar architecture remains the isolation capacitance that is around 13pF, which is limiting for very fast switching WBG devices. The converter makes use of a 40V GaN input bridge that creates a very low level of losses. As a result, the maximum efficiency is 76.6%, and most losses are concentrated in the copper traces and the diodes of the output bridge. All in all, the power supply fulfills the output voltage specifications with a PCB-based system integration and using off-the shelf components.

References

[1] G. Regnat, P. Jeannin, G. Lefevre, J. Ewanchuk, D. Frey, S. Mollov, and J.P. Ferrieux, “Silicon Carbide Power Chip On Chip Module Based On Embedded Die Technology With Paralleled Dies,” in ECCE 2015, pp. 4913–4919.

[2] M. Kazanbas, A. Schittler, S. Araújo, and P. Zacharias, “High-Side Driving under High-Switching Speed : Technical Challenges and Testing Methods,” in PCIM Europe 2015, 2015, no. May, pp. 19–21.

[3] B. Chen, “Fully Integrated Isolated DC-DC Converter Using Micro-Transformers,” in APEC 2008, pp. 335–338.

[4] O. Deleage, J. Crebier, M. Brunet, Y. Lembeye, and H. T. Manh, “Design and Realization of Highly Integrated Isolated,” vol. 47, no. 2, pp. 930–938, 2011.

[5] C. Mathuna and N. Wang, “Review of integrated magnetics for power supply on chip (PwrSoC),” IEEE Transactions on Power Electron., vol. 27, no. 11, pp. 4799–4816, 2012.

[6] E. Haddad, C. Martin, C. Joubert, and B. Allard, “Planar , Double-layer Magnetic Inductors for Low Power , High Frequency DC-DC Converters,” pp. 2–5.

[7] J. Park, L. Lagorce, and M. Allen, “Ferrite-based integrated planar inductors and transformers fabricated at low temperature,” Magn. IEEE Trans. 1997.

[8] S. Tang, S. Hui, and H. Chung, “A low-profile power converter using printed-circuit board (PCB) power transformer with ferrite polymer composite,” IEEE Trans. Power Electron., vol. 16, no. 4, pp. 493–498, 2001.

[9] J. Lu, H. Jia, A. Arias, X. Gong, and Z. J. Shen, “On-Chip Bondwire Magnetics with Ferrite-Epoxy Glob Coating for Power Systems on Chip,” Int. J. Power Manag. Electron., vol. 2008, pp. 1–9, 2008.

[10] J. Lu, S. Member, H. Jia, X. Wang, K. Padmanabhan, and W. G. Hurley, “Modeling , Design , and Characterization of Multiturn Bondwire Inductors With Ferrite Epoxy Glob Cores for Power Supply System-on-Chip or System-in-Package Applications,” vol. 25, no. 8, pp. 2010–2017, 2010.

[11] J. Y. Park and M. G. Allen, “Development of magnetic materials and processing techniques applicable to integrated micromagnetic devices,” J. Micromechanics Microengineering, vol. 8, no. 4, pp. 307–316, Dec. 1998.

[12] Z. J. Shen, J. Lu, X. Cheng, H. N. Jia, and X. G. Ng, “On-Chip Bondwire Inductor with Ferrite-Epoxy Coating: A Cost-Effective Approach to Realize Power Systems on Chip,” 2007 IEEE Power Electron. Spec. Conf., pp. 1599–1604, 2007.